JOURNAL OF PHYSICAL ORGANIC CHEMISTRY
J. Phys. Org. Chem. 2004; **17:** 707–714
Published online in Wiley InterScience (www.interscience.wiley.com). DOI: 10.1002/poc.740

Ortho effects and cross interaction correlations for the mechanisms of cholesterol esterase inhibition by aryl carbamates

Gialih Lin,* Yu-Chen Liu, Yon-Gi Wu and Yu-Ru Lee

Department of Chemistry, National Chung-Hsing University, Taichung 402, Taiwan

Received 23 February 2003; revised 4 November 2003; accepted 5 December 2003

ABSTRACT: *Ortho*-substituted phenyl-*N*-butyl carbamates (**1–11**) were synthesized to evaluate the inhibition mechanisms of porcine pancreatic cholesterol esterase. All carbamate inhibitors act as the active site-directed pseudo substrate inhibitors of the enzymes. The logarithms of dissociation constant (K_i), carbamylation constant (k_2) and bimolecular inhibition constant (k_i) multiply linearly correlate with the Hammett substituent constant (σ), the Taft–Kutter–Hansch *ortho* steric constant (E_S), and the Swan–Lupton–Hansch *ortho* polar constant (F). For the $-\log K_i$, $\log k_2$ and $\log k_i$ correlations, the reaction constant for ordinary polar effect (ρ), the intensity factor to *ortho* steric constant (δ) and the intensity factor to *ortho* polar constant (f) are 0.7, −0.07, and 0.5; 0.5, 0.04 and −0.5; and 1.1, −0.03 and 0.0, respectively. The cross interaction reaction constant (ρ_{XR}) for the $-\log k_i-$, $\log k_2-$ and $\log k_i-\sigma-\alpha\sigma^*-\alpha\sigma\sigma^*$ correlations are 3, −2, and 1, respectively. The K_i step may be composed of the following two steps: (1) protonation of carbamates **1–11** and (2) the pseudo-*trans* to pseudo-*cis* conformation change of protonated carbamates **1–11** due to a large ρ_{XR} value of 3 and formation of the enzyme-protonated carbamates **1–11** tetrahedral intermediate. The k_2 step involves departure of the leaving group, which is protonated by the active site histidine of the enzyme, from the tetrahedral intermediate to solution and formation of the carbamyl enzyme. Moreover, the distances between the carbamate and phenyl groups in all transition states of inhibition reactions are relatively short owing to large $|\rho_{XR}|$ values. The K_i step shows little *ortho* steric enhancement effect; moreover, the k_2 step shows little *ortho* steric inhibition effect. Copyright © 2004 John Wiley & Sons, Ltd.

KEYWORDS: *ortho* effects; cross interaction correlations; cholesterol esterase; carbamate inhibitors

INTRODUCTION

Pancreatic cholesterol esterase (CEase, EC 3.1.1.13), also known as bile salt-stimulated lipase, pancreatic carboxyl ester lipase, pancreatic lysophospholipase, non-specific lipase, functions in the hydrolysis of dietary cholesterol esters and other dietary esters.[1] In addition to cholesterol esters, triacylglycerols, phospholipids and vitamin esters are also substrates of CEase.[2,3] Two x-ray structures of CEase have been reported recently.[4,5] Although different bile salt-activation mechanisms have been proposed, the active site of CEase is similar to that of lipases.[6–8]

Recently, there has been increased interest in CEase and lipases owing to the correlation between enzymatic activity *in vivo* and absorption of dietary cholesterol[9,10] and the use of orlistat (Xenical). Orlistat, whose original mechanism of action consists of the selective inhibition of gastrointestinal lipases, has been commercialized for the treatment of obesity.[11,12] It has also been demonstrated that CEase is involved directly in lipoprotein metabolism, in that the enzyme catalyzes the conversion of large low-density lipoprotein to smaller, denser, more cholesterol ester-rich lipoproteins, and that the enzyme may regulate serum cholesterol levels.[13] Both CEase and lipase share the same catalytic mechanism as serine proteases[14] in that they have a Ser–His–Asp (Glu) catalytic triad that is involved in nucleophilic and general acid–base catalysis and a neighboring oxyanion hole (OAH), the hydrogen bonding peptide NH functions of Gly and Ala, that stabilizes the incipient carbonyl C—O^- of the ester function during turnover. Both CEase and lipase may well be expected to be inhibited by the same classes of mechanism-based inhibitors. In the presence

**Correspondence to:* G. Lin, Department of Chemistry, National Chung-Hsing University, Taichung 402, Taiwan.
E-mail: gilin@dragon.nchu.edu.tw
Contract/grant sponsor: National Science Council of Taiwan.

Abbreviations: ACS, alkyl chain binding site; CEase, cholesterol esterase; δ, intensity factor to *ortho* steric constant or NMR chemical shift in ppm; ES, esteratic site; E_s, Taft–Kutter–Hansch *ortho* steric constant; F, Swan–Lupton–Hansch *ortho* polar constant; f, intensity factor to *ortho* polar constant; k_2, carbamylation constant; k_3, decarbamylation constant; K_i, inhibition or dissociation constant; K_i', virtual inhibition or dissociation constant of the enzyme-protonated carbamate tetrahedral intermediate; OAH, oxyanion hole; PNPB, *p*-nitrophenyl butyrate; QSAR, quantitative structure–activity relationship; ρ, reaction constant for ordinary polar effect; SACS; second alkyl chain binding site; TFA, trifluoroacetophenone.

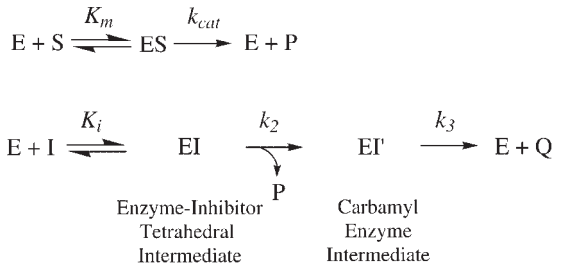

Scheme 1. Kinetic scheme for pseudo substrate inhibitions of CEase in the presence of substrate

of substrate, the CEase inhibition by pseudo substrate inhibitors such as carbamates have been proposed (Scheme 1).[15–22] Since the inhibition follows first-order kinetics over the observed time period for the steady-state kinetics, the rate of hydrolysis of EI′ must be significantly slower than the rate of formation of EI′ ($k_2 \gg k_3$).[23] Therefore, values of K_i and k_2 can be calculated from the equation.[15]

$$k_{\text{app}} = k_2[\text{I}]/(K_i(1 + [\text{S}]/K_m) + [\text{I}]) \qquad (1)$$

where k_{app} is the first-order rate constant and can be obtained according to Hosie's method.[15] The bimolecular rate constant, $K_i = k_2/K_i$, is related to overall inhibitory potency.

According to the x-ray structures of CEase and lipases,[4,5,7,8] CEase consists of at least five major binding sites:[20,21] (a) an alkyl chain binding site (ACS) that binds to the substrate alkyl chain, (b) an oxyanion hole (OAH) that stabilizes the tetrahedral intermediate, (c) an esteratic site (ES), comprised of the active site serine which attacks the ester carbonyl, (d) a leaving group hydrophobic binding site, the peripheral site and/or the second alkyl chain or group binding site (SACS) that binds to the cholesterol part of cholesterol ester or the second fatty acid chain of triacylglyceols, which is relatively larger than ACS, and (e) a leaving group hydrophilic binding site that binds to the hydrophilic part of the leaving group and is located at the opposite direction of ACS.

Quantitative structure–activity relationships (QSARs) represent an attempt to correlate structural properties of compounds with activities or reactivities.[24–26] These chemical descriptors, which include parameters to account for hydrophobicity, electronic, inductive or polar properties and steric effects, are determined empirically or by calculations. Many biological activities and chemical reactivities are correlated with the Hammett equation:[24–26]

$$\log k = h + \rho\sigma \qquad (2)$$

where h, ρ and σ are $\log k_0$, the reaction constant (or intensity factor for inductive effect) and the Hammett substituents constant, respectively. Also, *meta*- and *para*-substituted compounds generally correlate well but *ortho*-substituted compounds do not.[25] *Ortho* problems, due to complications from direct steric and polar effects, are not generally applicable.[27] According to Fujita and Nishioka's suggestion, the total *ortho* effect is composed of the ordinary polar effect, the *ortho* steric effect and the *ortho* polar effect:[25,27]

$$\log k = h + \rho\sigma + \delta E_S + fF \qquad (3)$$

where h, ρ, σ, E_S, δ, f and F are $\log k_0$, the reaction constant for ordinary polar effect, the Hammett substituent constant, the Taft–Kutter–Hansch *ortho* steric constant, the intensity factor to *ortho* steric constant, the intensity factor to *ortho* polar constant and the Swain–Lupton–Hansch *ortho* polar constant, respectively.

Cross interaction correlations for the CEase inhibitions by *meta*- and *para*-substituted phenyl-*N*-butylcarbamates (**13**) and *p*-nitrophenyl-*N*-substituted carbamates (**12**) with Eqn (4)[28,29] reveal that the carbamate O—C(O)—N—R geometries in the transition states of all inhibition reactions retain in the pseudo-*trans* conformations:

$$\log k = h + \rho\sigma + \rho^*\alpha\sigma^* + \rho_{XR}\sigma\alpha\sigma^* \qquad (4)$$

where h, ρ, σ, ρ^*, σ^*, ρ_{XR} and α are $\log k_0$, the reaction constant for the substituted phenyl part (varied X, Fig. 1) of the inhibitor, the Hammett substituent constant of X, the reaction constant for the substituted carbamate part (varied R, Fig. 1) of the inhibitor, the Taft substituent constant of R, the cross interaction constant and the weighing factor for the Hammett–Taft cross interaction term ($\alpha = 1$ for the Hammett substituent X; $\alpha = 2.54$ for the Taft substituent R), respectively.[28] Moreover, the distance between X and R substituents in the transition state of the reaction is inversely proportional to $|\rho_{XR}|$.[29]

Aryl carbamates, such as *meta*- and *para*-substituted phenyl-*N*-substituted carbamates (**12** and **13**) (Fig. 1), are characterized as the pseudo substrate inhibitors of CEase and show the Hammett[16,18,21] and Taft–Ingold types[17,20,21] of correlations. In this work, *ortho*-substituted phenyl-*N*-butyl carbamates (**1**–**11**) (Fig. 1) were synthesized to explore the *ortho* effects for the pre-steady-state CEase inhibition and the cross interaction correlations with *p*-nitrophenyl-*N*-substituted carbamates (**12**) (Fig. 1).

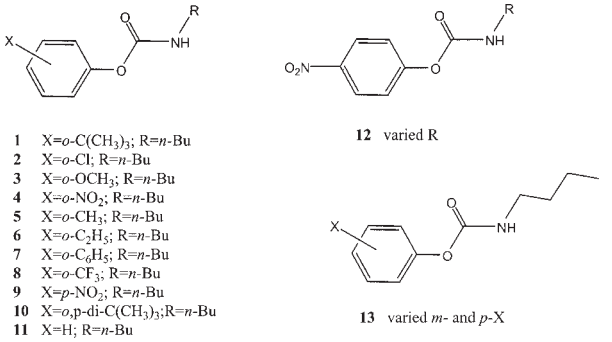

Figure 1. Structures of carbamates **1**–**12**

Table 1. *Ortho* substituent constants and inhibition constants for CEase-catalyzed hydrolysis of PNPB in the presence of carbamates **1–11**

Inhibitor	Substituent	σ[a]	E_S[a]	F[b]	k_2 (10^{-4} s^{-1})[c]	K_i (μM)[c]	k_i (10^3 M^{-1} s^{-1})[d]
1	*o*-*t*-Bu	−0.20	−2.78	−0.07	15.8 ± 0.4	3.2 ± 0.3	0.5 ± 0.1
2	*o*-Cl	0.23	−0.97	0.41	16.5 ± 0.8	2.2 ± 0.4	0.8 ± 0.2
3	*o*-OMe	−0.27	−0.55	0.26	7.0 ± 0.05	7 ± 1	0.10 ± 0.02
4	*o*-NO_2	0.78	−2.52	0.67	17.6 ± 0.7	0.8 ± 0.3	2.2 ± 0.4
5	*o*-CH_3	−0.17	−1.24	−0.04	20.3 ± 0.8	7 ± 1	0.30 ± 0.02
6	*o*-C_2H_5	−0.15	−1.31	−0.05	13.8 ± 0.3	7 ± 1	0.20 ± 003
7	*o*-Ph	−0.01	−1.01	0.08	11.7 ± 0.8	5 ± 1	0.23 ± 0.03
8	*o*-CF_3	0.54	−2.40	0.38	9.5 ± 0.1	0.7 ± 0.1	1.4 ± 0.2
9	*p*-NO_2	0.78	0	0	38 ± 2	2.6 ± 0.3	1.5 ± 0.1
10	*o*,*p*-Di-*t*-Bu	−0.4	−2.78	−0.07	7.5 ± 0.7	18 ± 3	0.04 ± 0.02
11	H	0	0	0	16.8 ± 0.9	5 ± 1	0.32 ± 0.02

[a] Hydrogen is taken as standard. These values are calculated from Refs. 24–26.
[b] Taken from Ref. 27.
[c] Obtained from fitting the k_{app} values to Eqn (1).
[d] $k_i = k_2/K_i$.

RESULTS

Carbamates **1–11** (Fig. 1) are characterized as the pseudo substrate inhibitors of CEase because the inhibitors are time dependent, the inhibitions follow first-order kinetics and the enzyme activities recover with a competitive inhibitor, trifluoroacetophenone (TFA).[15–22] The *ortho* substituent constants and inhibition constants for the CEase-catalyzed hydrolysis of *p*-nitrophenyl butyrate (PNPB) by carbamates **1–11** are summarized in Table 1.

Correlations of δ_{NH}, $\delta_{C=O}$, $-\log K_i$, $\log k_2$ and $\log k_i$ with the Hammett equation [Eqn (2)] are poor (Table 2). These correlations are improved after addition of the Taft–Kutter–Hansch steric constant, E_S, to the correlation parameters (Table 2). Multiple correlations with three parameters, σ, E_S and F [(Eqn (3)],[25,27] are much improved (Table 2). The bimolecular rate constant, $k_i = k_2/K_i$, is related to overall inhibitory potency.[15–22] The pK_a values of carbamates **1–12** are correlated with the Hammett equation [Eqn (2)] (Table 2).[21] The $-\log K_i'$ values are well correlated with Eqn (3) (Table 2), where the virtual inhibition constant, $K_i' = K_b K_i$, is the dissociation constant of the enzyme-protonated carbamate tetrahedral intermediate.

The results for the cross interaction correlation between the *ortho*-substituted carbamates **1–11** and 4-nitrophenyl-*N*-substituted carbamates (**12**) (Fig. 1) are summarized in Table 3. The $|\rho_{XR}|$ values for the cross interaction between *ortho*-substituted carbamates **1–11** and carbamates **12** are larger than those between

Table 2. QSAR results for NMR chemical shifts of carbamates **1–11** and the inhibition constants for the inhibitions of CEase by carbamates **1–11**

	h	ρ	δ	f	R
δ_{NH}^a	5.12 ± 0.03	0.27 ± 0.09	—	—	0.718
δ_{NH}^b	5.13 ± 0.07	0.3 ± 0.1	0.01 ± 0.04	—	0.719
δ_{NH}^c	5.07 ± 0.07	0.0 ± 0.2	0.00 ± 0.03	0.4 ± 0.3	0.813
$\delta_{C=O}^a$	154.09 ± 0.07	−1.3 ± 0.2	—	—	0.913
$\delta_{C=O}^b$	154.1 ± 0.2	−1.3 ± 0.2	−0.01 ± 0.09	—	0.913
$\delta_{C=O}^c$	154.3 ± 0.1	−0.5 ± 0.3	0.01 ± 0.06	−1.3 ± 0.4	0.969
$\text{Log } K_b^d$	4.00 ± 0.06	−2.5 ± 0.1	—	—	0.989
$-\text{Log } K_i'^e$	9.2 ± 0.2	3 ± 1	−0.07 ± 0.07	0.5 ± 0.3	0.906
$-\text{Log } K_i^a$	5.35 ± 0.07	0.8 ± 0.2	—	—	0.847
$-\text{Log } K_i^b$	5.2 ± 0.1	0.9 ± 0.2	−0.10 ± 0.07	—	0.884
$-\text{Log } K_i^c$	5.2 ± 0.1	0.7 ± 0.2	−0.07 ± 0.07	0.5 ± 0.3	0.912
$\text{Log } k_2^a$	−2.87 ± 0.06	0.3 ± 0.1	—	—	0.559
$\text{Log } k_2^b$	−2.78 ± 0.09	0.3 ± 0.1	0.07 ± 0.05	—	0.654
$\text{Log } k_2^c$	−2.76 ± 0.08	0.5 ± 0.1	0.04 ± 0.05	−0.5 ± 0.2	0.811
$\text{Log } k_i^a$	2.47 ± 0.07	1.1 ± 0.2	—	—	0.904
$\text{Log } k_i^b$	2.4 ± 0.1	1.1 ± 0.2	−0.03 ± 0.07	—	0.906
$\text{Log } k_i^c$	2.4 ± 0.1	1.1 ± 0.3	−0.03 ± 0.08	0.0 ± 0.1	0.906

[a] Correlation with σ [Eqn (2)] for carbamates **1–11**.
[b] Correlation with σ and E_S for carbamates **1–11**.
[c] Correlation with σ, E_S and F [Eqn (3)] for carbamates **1–11**.
[d] Correlation with σ, E_S and F [Eqn (3)] for carbamates **1–11** and *meta*- and *para*-substituted phenyl-*N*-butylcarbamates.
[e] $1/K_i = K_b\ (1/K_i')$.

Table 3. Cross interaction correlation results for the CEase inhibitions by *ortho*-substituted phenyl-*N*-butylcarbamates (**1–11**) and *p*-nitrophenyl-*N*-substituted carbamates (**12**)

Parameter[a]	$-\log K_i$	$\log k_2$	$\log k_i$
ρ^*	-2.4 ± 0.8	-0.9 ± 0.1	-1.2 ± 0.8
ρ	1.1 ± 0.3	0.0 ± 0.3	1.1 ± 0.3
ρ_{XR}[b]	3 ± 1	-2 ± 1	1 ± 1
h	4.6 ± 0.2	-2.4 ± 0.3	2.2 ± 0.3
R[c]	0.827	0.728	0.872

[a] Correlation of the $-\log K_i$, $\log k_2$ and $\log k_i$ values for the CEase inhibitions by *ortho*-substituted phenyl-*N*-butylcarbamates (**1–11**) and *p*-nitrophenyl-*N*-substituted carbamates (**12**)[17,21,28] on Eqn (4).[28,29]
[b] Cross interaction constant.[29]
[c] Correlation coefficient.

para- and *meta*-substituted carbamates and carbamates **12**.[28] In other words, the distances between X and R in the transition states for the CEase inhibitions by *ortho* substituted carbamates are much shorter than those inhibitions by *para*- and *meta*-substituted carbamates. Therefore, this result confirms that the carbamate inhibitor conformations during all inhibition reactions retain the pseudo-*cis* conformations.[28]

DISCUSSION

Like *meta*- and *para*-substituted phenyl-*N*-butylcarbamates[16–18,21] and 1,1′-bi-2-naphthyl- 2,2′-di-*N*- butylcarbamate,[19] carbamates **1–11** are characterized as the pseudo substrate inhibitors of CEase (Scheme 1 and Table 1) and show the same kinetic behavior. Therefore, the leaving group binding site of the enzyme is large enough to adapt to extremely bulky *ortho* substituents such as 1-naphthyl, *tert*-butyl, and phenyl.

The f value of 0.4 for the δ_{NH}–σ–E_S–F correlation suggests that the N—H bonds of carbamates **1–11** polarize to generate a partial negative charge on nitrogen under the NMR conditions; moreover, the f value of –1.3 for the $\delta_{C=O}$–σ–E_S–F correlation suggests that the C═O bonds of carbamates **1–11** polarize to generate a partial positive charge on carbon under the NMR conditions.

A three-step CEase inhibition mechanism by carbamates **1–11** is proposed (Fig. 2). The first step (K_b) is the pre-equilibrium protonation of carbamates **1–11**. The second step (K_i') is formation of the enzyme-protonated carbamate tetrahedral intermediate. The third step (k_2) is formation of the carbamyl enzyme intermediate and release of the substituted phenol product.

K_b step

For the K_b step, carbamates **1–11** like carbamates **13** and **12**,[21,28] are bases (Table 2) and are protonated in aqueous solution outside the enzyme active site (pH 7). From the cross interaction correlation results,[28] the

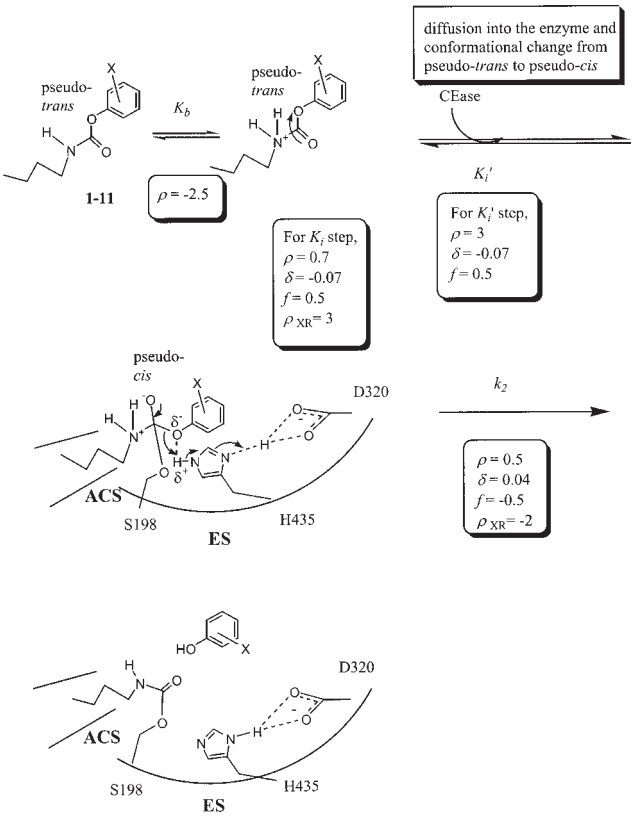

Figure 2. The proposed CEase inhibition mechanisms by carbamates **1–11**. The K_b step is protonation of carbamates **1–11**. The ρ value for the $\log K_b$–σ correlation is -2.5. Therefore, protonated carbamates **1–11** are more positively charged than carbamates **1–11**. The O—C(O)—N—R geometries of carbamates **1–11** and protonated of carbamates **1–11** are all pseudo-*trans* conformations. The K_i' step is formation of the enzyme–protonated carbamate tetrahedral intermediate. The ρ_{XR} value for the $-\log K_i$–σ–$\alpha\sigma^*$–$\alpha\sigma\sigma^*$ cross interaction correlation is 3. Hence the O—C(O)—N—R geometry of the tetrahedral intermediate changes to the pseudo-*cis* conformation. Values of ρ, δ, and f for the $-\log K_i'$–σ–E_s–F correlation are 3, -0.07 and 0.5, respectively. The k_2 step is formation of the carbamyl enzyme intermediate. The ρ_{XR} value for the $\log k_2$–σ–$\alpha\sigma^*$–$\alpha\sigma\sigma^*$ cross interaction correlation is -2. Hence, the O—C(O)—N—R geometry for the transition state which leads to the carbamyl enzyme retains in the pseudo-*cis* conformation. Values of ρ, δ and f for the k_2 step are 0.5, 0.04 and -0.5, respectively

O—C(O)—N—R geometries of carbamates **1–11** and protonated carbamates **1–11** are in the pseudo-*trans* conformations (Fig. 2). The excellent $\log K_b$–σ correlation (Table 2) indicates that the K_b step is insensitive to *ortho* steric and polar effects because the *ortho* substituents are far away from the carbamate nitrogen reaction centers.

K_i' step

For the K_i' step, the ρ value of 3 for the $-\log K_i'$–σ–E_S–F correlation (Table 2) suggests that the enzyme–protonated carbamate tetrahedral intermediates are more

negative charges than protonated carbamates **1–11** (Fig. 2). There is little *ortho* steric enhancement effect in the CEase inhibitions by protonated carbamates **1–11** owing to a negative, small δ value (-0.07) for this correlation (Table 2). Therefore, the enzyme active site prefers to adapt bulky *ortho* substituents of the inhibitors. Since the f value for the K_b step is zero, the f value (0.5) for the K_i' step should be identical with that for the K_i step (discussed later). The carbamate O—C(O)—N—R geometry for the K_i' step changes from the pseudo-*trans* to pseudo-*cis* conformation (Fig. 2, discussed later).

K_i step

The K_i step consists of the K_b and K_i' steps. The ρ value of 0.7 for the $-\log K_i$–σ–E_S–F correlation (Table 2) suggests that the enzyme–protonated carbamate tetrahedral intermediates are slightly more negative charges than carbamates **1–11** (Fig. 2). There is also little *ortho* steric enhancement effect in the CEase inhibitions by carbamates **1–11** (Table 2). For the alkaline hydrolyses of benzoyl esters and amides, the f values are very similar, the average being 1.1.[27] The f value of 0.5 for the K_i or K_i' step is less than 1.1 because the distance of the carbamate carbonyl reaction center to the phenyl ring is longer than that of the benzoyl carbonyl reaction center to the phenyl ring. For phenylacetic acid ester formation and hydrolysis, the f value is almost unchanged regardless of the catalytic condition of reactions, being -0.2 to -0.4.[27] Therefore, the carbamate ether oxygen probably transimits the proximity effect much easier than the phenylacetic methylene. The ρ_{XR} value of 3 for the $-\log K_i$–σ–$\alpha\sigma^*$–$\alpha\sigma\sigma^*$ cross interaction correlation (Table 3) indicates that the distance between X and R substituents (Fig. 1) in the transition state of the K_i step is relatively short and that the carbamate O—C(O)—N—R geometry in the tetrahedral intermediate changes to the pseudo-*cis* conformation (Fig. 2).[28] Moreover, this ρ_{XR} value is greater than that for the cross interaction between carbamates **13** and **12** (Fig. 1) ($\rho_{XR} = 2$).[28] Apparently, the distance between X and R substituents for the pseudo-*cis* conformation in the *ortho*-substituted carbamate tetrahedral intermediate is shorter than that in the *meta*- and *para*-substituted intermediates.

k_2 step

For the k_2 step, the ρ value for the $\log k_2$–σ–E_S–F correlation is 0.5 (Table 2). Therefore, the substituted phenol product for this step is more negatively charged than the tetrahedral intermediate. The bulky *ortho* substituents of the tetrahedral intermediate slightly inhibit the CEase inhibition reactions owing to a small positive δ value (0.04) (Table 2). Hence the leaving group binding site of CEase slightly prefers to adapt less bulky *ortho*-substituted phenol. The f value in this correlation is about -0.5 (Table 2), which is not the value for formation of the substituted phenoxide ion ($f = 2.6$).[27] Therefore, the pseudo leaving groups, phenoxide ions, are assumed to be protonated by His-435 of the enzyme soon after their formation (Fig. 2). Hence the true leaving group for this reaction is substituted phenol. Therefore, the O—C(O)—N—R geometry of the tetrahedral intermediate must be retained in the pseudo-*cis* conformation in order to obtain the proton from His345 of the enzyme (Fig. 2). The f value for the ^{1}H NMR spectra of substituted phenols in DMSO is about 0.6, which may indicate the *ortho* polar effect for a polarization process of the hydroxyl bond (Fig. 3).[27] Accordingly, the f value of -0.5 suggests that the retro-polarization process for the hydroxyl bond (Fig. 3) strongly resembles the formation mechanism for substituted phenol in the k_2 step (Fig. 2). The ρ_{XR} value of -2 for the $-\log k_2$–σ–$\alpha\sigma^*$–$\alpha\sigma\sigma^*$-correlation (Table 3) indicates that the distance between X and R substituents (Fig. 1) in the transition state of the k_2 step is relatively short and that the carbamate O—C(O)—N—R geometry in the transition state of this step retains in the pseudo-*cis* conformation (Fig. 2).[28]

k_i step

The k_i step consists of both K_i (consists of K_b and K_i') and k_2 steps. The f value of 0.0 for the $\log K_i$–σ–E_S–F correlation (Table 2) indicates that the sum of both f values for the $\log K_i$–σ–E_S–F ($f = 0.5$) and $\log k_2$–σ–E_S–F ($f = -0.5$) correlations. Moreover, as most data for k_i (Tables 1–3) can also be calculated from those for K_i and k_2, this confirms that the k_i step consists of both K_i and k_2 steps. However, ρ^* value of the $\log k_i$–σ–$\alpha\sigma^*$–$\alpha\sigma\sigma^*$ correlation differs slightly from the sum of that of $-\log K_i$– and $\log k_2$–σ–$\alpha\sigma^*$–$\alpha\sigma\sigma^*$ correlations probably because these correlations are poor and *ortho* effects are not taken into account in Eqn (4) (Table 3).

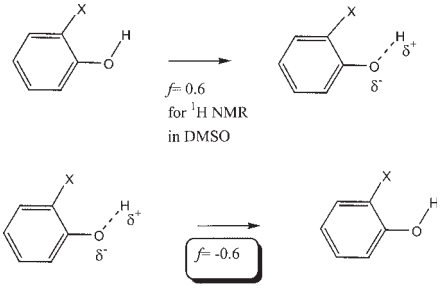

Figure 3. Polarization and retro-polarization processes of the substituted phenol hydroxyl bonds. The polarization process (top) of the substituted phenol hydroxyl bond generates a partial negative charge at oxygen in the NMR condition. The f value for the polarization process is 0.6 from NMR spectra. The retro-polarization process (bottom) of the substituted phenol hydroxyl bond neutralizes the partial negative charge at oxygen. The f value for the retro-polarization process should be -0.6. The retro-polarization process of substituted phenol in aqueous solution mimics the k_2 step (Fig. 2) ($f = -0.5$)

EXPERIMENTAL

Materials

CEase from porcine pancreas and *p*-nitrophenyl butyrate (PNPB) were obtained from Sigma; other chemicals were obtained from Aldrich. Silica gel used in liquid chromatography (Licorpre silica 60, 200–400 mesh) and thin-layer chromatographic plates (60 F_{254}) were obtained from Merck. All other chemicals were of the highest purity available commercially.

Instrumental methods

^{1}H and ^{13}C NMR spectra were recorded at 400 and 100 MHz, respectively, on a Varian Gemini 400 spectrometer. All steady-state kinetic data were obtained using a UV–visible spectrophotometer (HP 8452 or Beckman DU-650) with a cell holder circulated with a water-bath.

Data reduction

Origin (version 6.0) was used for linear, non-linear and multiple linear least-squares regression analyses.

Steady-state enzyme kinetics

The CEase inhibition was assayed by Hosie's method.[15] The temperature was maintained at 25.0 ± 0.1 °C by a refrigerated circulating water-bath. All inhibition reactions were performed in sodium phosphate buffer (1 ml, 0.1 M, pH 7.0) containing NaCl (0.1 M), CH_3CN (2 vol%), Triton X-100 (0.5 wt%), substrate (0.2 mM) and varying concentration of inhibitors. Requisite volumes of stock solutions of substrate and inhibitors in acetonitrile were injected into the reaction buffer via a pipet. CEase was dissolved in sodium phosphate buffer (0.1 M, pH 7.0). First-order rate constants (k_{app}) for inhibition were determined as described by Hosie *et al.*[15] The K_i and k_2 values were obtained by fitting k_{app} and [I] to Eqn (1) by non-linear least-squares regression analyses.[15–22] Duplicate sets of data were collected for each inhibitor concentration.

Synthesis of carbamates

Carbamates **1–11** were prepared by condensation of the corresponding phenol with *n*-butyl isocyanate in the presence of a catalytic amount of pyridine in toluene. All compounds were purified by liquid chromatography on silica gel and characterized by ^{1}H and ^{13}C NMR spectrometry and high-resolution mass spectrometry (HRMS).

*o-tert-Butylphenyl-N-butylcarbamate (**1**).* ^{1}H NMR ($CDCl_3$, 400 MHz), δ (ppm) 0.96 (t, $J = 7$ Hz, 3H, $CH_2CH_2CH_3$), 1.32 [s, 9H, $C(CH_3)_3$], 1.38 (sextet, $J = 7$ Hz, 2H, $CH_2CH_2CH_3$), 1.58 (quintet, $J = 7$ Hz, 2H, $CH_2CH_2CH_3$), 3.31 (q, $J = 7$ Hz, 2H, $NHCH_2$), 5.02 (br s, 1H, NH), 7.04–7.37 (m, 4H, aromatic *H*). ^{13}C NMR ($CDCl_3$, 100 MHz), δ (ppm) 13.84 ($CH_2CH_2CH_3$), 19.98 ($CH_2CH_2CH_3$), 30.34 [$C(CH_3)_3$], 32.09 ($CH_2CH_2CH_3$), 34.23 [$C(CH_3)_3$], 41.06 ($NHCH_2$), 124.05, 125.04, 126.63, 126.76 (phenyl CH), 141.08 (phenyl *C*-1), 149.35 (phenyl *C*-2), 154.42 (C=O). HRMS, calculated for $C_{15}H_{23}NO_2$ 249.1729, found 249.1733.

*o-Chlorophenyl-N-butylcarbamate (**2**).* ^{1}H NMR ($CDCl_3$, 400 MHz), δ (ppm) 0.92 (t, $J = 7$ Hz, 3H, $CH_2CH_2CH_3$), 1.37 (sextet, $J = 7$ Hz, 2H, $CH_2CH_2CH_3$), 1.52 (quintet, $J = 7$ Hz, 2H, $CH_2CH_2CH_3$), 3.23 (q, $J = 7$ Hz, 2H, $NHCH_2$), 5.37 (br s, 1H, NH), 7.12–7.41 (m, 4H, aromatic *H*); ^{13}C NMR ($CDCl_3$, 100 MHz), δ (ppm) 13.72 ($CH_2CH_2CH_3$), 19.84 ($CH_2CH_2CH_3$), 31.77 ($CH_2CH_2CH_3$), 41.04 ($NHCH_2$), 123.92, 126.23, 127.32, 129.87 (phenyl CH), 127.08 (phenyl *C*-2), 146.92 (phenyl *C*-1), 153.35 (C=O). HRMS, calculated for $C_{11}H_{14}NO_2Cl$ 227.0713, found 227.0721.

*o-Methoxyphenyl-N-butylcarbamate (**3**).* ^{1}H NMR ($CDCl_3$, 400 MHz), δ (ppm) 0.94 (t, $J = 7$ Hz, 3H, $CH_2CH_2CH_3$), 1.39 (sextet, $J = 7$ Hz, 2H, $CH_2CH_2CH_3$), 1.57 (quintet, $J = 7$ Hz, 2H, $CH_2CH_2CH_3$), 3.27 (q, $J = 7$ Hz, 2H, $NHCH_2$), 3.85 (s, 3H, OCH_3), 5.05 (br s, 1H, NH), 6.91–7.20 (m, 4H, aromatic *H*). ^{13}C NMR ($CDCl_3$, 100 MHz), δ (ppm) 13.82 ($CH_2CH_2CH_3$), 19.93 ($CH_2CH_2CH_3$), 31.93 ($CH_2CH_2CH_3$), 41.07 ($NHCH_2$), 55.88 (OCH_3), 112.22, 120.53, 123.12, 126.17 (phenyl CH), 139.83 (phenyl *C*-2), 151.47 (phenyl *C*-1), 154.17 (C=O). HRMS, calculated for $C_{12}H_{17}NO_3$ 223.1208, found 223.1211.

*o-Nitrophenyl-N-butylcarbamate (**4**).* ^{1}H NMR ($CDCl_3$, 400 MHz), δ (ppm) 0.94 (t, $J = 7$ Hz, 3H, $CH_2CH_2CH_3$), 1.32 (sextet, $J = 7$ Hz, 2H, $CH_2CH_2CH_3$), 1.51 (quintet, $J = 7$ Hz, 2H, $CH_2CH_2CH_3$), 3.28 (t, $J = 7$ Hz, 2H, $NHCH_2$), 5.28 (br s, 1H, NH), 7.22–8.05 (m, 4H, aromatic *H*). ^{13}C NMR ($CDCl_3$, 100 MHz), δ (ppm) 13.70 ($CH_2CH_2CH_3$), 19.80 ($CH_2CH_2CH_3$), 32.03 ($CH_2CH_2CH_3$), 41.20 ($NHCH_2$), 125.40, 125.70, 125.90, 134.20 (phenyl CH), 142.10 (phenyl *C*-2), 144.20 (phenyl *C*-1), 153.10 (C=O). HRMS, calculated for $C_{11}H_{14}N_2O_4$ 238.0954, found 238.0959.

*o-Methylphenyl-N-butylcarbamate (**5**).* ^{1}H NMR ($CDCl_3$, 400 MHz), δ (ppm) 0.94 (t, $J = 7$ Hz, 3H, $CH_2CH_2CH_3$), 1.37 (sextet, $J = 7$ Hz, 2H, $CH_2CH_2CH_3$), 1.54 (quintet, $J = 7$ Hz, 2H, $CH_2CH_2CH_3$), 2.21 (s, 3H, *o*-CH_3), 3.25 (q, $J = 7$ Hz, 2H, $NHCH_2$), 5.09 (br s, 1H, NH), 7.05–7.25 (m, 4H, aromatic *H*). ^{13}C NMR ($CDCl_3$, 100 MHz), δ (ppm)

13.81 ($CH_2CH_2CH_3$), 16.16 (*o*-CH_3), 19.96 ($CH_2CH_2CH_3$), 32.00 ($CH_2CH_2CH_3$), 41.00 ($NHCH_2$), 122.02, 125.34, 126.58, 130.77 (phenyl *C*H), 130.42 (phenyl *C*-2), 149.29 (phenyl *C*-1), 154.24 (*C*=O). HRMS, calculated for $C_{12}H_{17}NO_2$ 207.1260, found 207.1252.

*o-Ethylphenyl-N-butylcarbamate (**6**).* ^{1}H NMR ($CDCl_3$, 400 MHz), δ (ppm) 0.94 (t, $J = 7$ Hz, 3H, $CH_2CH_2CH_3$), 1.19 (t, 3H, $J = 7$ Hz, *o*-CH_2CH_3), 1.37 (sextet, $J = 7$ Hz, 2H, $CH_2CH_2CH_3$), 1.54 (quintet, $J = 7$ Hz, 2H, $CH_2CH_2CH_3$), 2.59 (q, $J = 7$ Hz, 2H, *o*-CH_2CH_3), 3.24 (q, $J = 7$ Hz, 2H, $NHCH_2$), 5.10 (br s, 1H, N*H*), 7.05–7.25 (m, 4H, aromatic *H*). ^{13}C NMR ($CDCl_3$, 100 MHz), δ (ppm) 13.79 ($CH_2CH_2CH_3$), 14.31 (*o*-CH_2CH_3), 19.93 ($CH_2CH_2CH_3$), 23.18 ($CH_2CH_2CH_3$), 31.98 (*o*-CH_2CH_3), 41.00 ($NHCH_2$), 122.28, 125.46, 126.49, 129.02 (phenyl *C*H), 136.07 (phenyl *C*-2), 148.81 (phenyl *C*-1), 154.49 (*C*=O). HRMS, calculated for $C_{13}H_{19}NO_2$ 221.1416, found 221.1407.

*o-Biphenyl-N-butylcarbamate (**7**).* ^{1}H NMR ($CDCl_3$, 400 MHz), δ (ppm) 0.96 (t, $J = 7$ Hz, 3H, $CH_2CH_2CH_3$), 1.32 (sextet, $J = 7$ Hz, 2H, $CH_2CH_2CH_3$), 1.43 (quintet, $J = 7$ Hz, 2H, $CH_2CH_2CH_3$), 3.19 (q, $J = 7$ Hz, 2H, $NHCH_2$), 5.03 (br s, 1H, N*H*), 7.27–7.51 (m, 9H, aromatic *H*). ^{13}C NMR ($CDCl_3$, 100 MHz), δ (ppm) 13.74 ($CH_2CH_2CH_3$), 19.73 ($CH_2CH_2CH_3$), 31.81 ($CH_2CH_2CH_3$), 40.78 ($NHCH_2$), 127.93, 128.13, 129.07, 123.10, 125.57, 127.01, 130.48 (phenyl *C*H), 134.82 (phenyl *C*-1′), 137.62 (phenyl *C*-2), 147.71 (phenyl *C*-1), 154.31 (*C*=O). HRMS, calculated for $C_{17}H_{19}NO_2$ 269.1416, found 269.1419.

*o-Trifluoromethylphenyl-N-butylcarbamate (**8**).* ^{1}H NMR ($CDCl_3$, 400 MHz), δ (ppm) 0.93 (t, $J = 7$ Hz, 3H, $CH_2CH_2CH_3$), 1.38 (sextet, $J = 7$ Hz, 2H, $CH_2CH_2CH_3$), 1.54 (quintet, $J = 7$ Hz, 2H, $CH_2CH_2CH_3$), 3.26 (q, $J = 7$ Hz, 2H, $NHCH_2$), 5.21 (br s, 1H, N*H*), 7.26–7.64 (m, 4H, aromatic *H*). ^{13}C NMR ($CDCl_3$, 100 MHz), δ (ppm) 13.75 ($CH_2CH_2CH_3$), 19.86 ($CH_2CH_2CH_3$), 31.84 ($CH_2CH_2CH_3$), 41.11 ($NHCH_2$), 122.10 (q, $^1J_{CF} = 180$ Hz, CF_3), 123.05 (q, $^2J_{CF} = 20$ Hz, phenyl *C*-2), 125.07, 126.48, 132.65 (phenyl *C*H), d, 148.38 (phenyl *C*-1), 153.42 (*C*=O). HRMS, calculated for $C_{12}H_{14}NO_2F_3$ 261.0977, found 261.0969.

*p-Nitrophenyl-N-butylcarbamate (**9**).* ^{1}H NMR ($CDCl_3$, 400 MHz), δ (ppm) 0.97 (t, $J = 7$ Hz, 3H, $CH_2CH_2CH_3$), 1.39 (sextet, $J = 7$ Hz, 2H, $CH_2CH_2CH_3$), 1.59 (quintet, $J = 7$ Hz, 2H, $CH_2CH_2CH_3$), 3.30 (q, $J = 7$ Hz, 2H, $NHCH_2$), 5.12 (br s, 1H, N*H*), 7.27–8.26 (m, 4H, aromatic *H*). ^{13}C NMR ($CDCl_3$, 100 MHz), δ (ppm) 13.78 ($CH_2CH_2CH_3$), 19.96 ($CH_2CH_2CH_3$), 31.81 ($CH_2CH_2CH_3$), 41.15 ($NHCH_2$), 121.75, 124.91 (phenyl *C*H), 144.45 (phenyl *C*-4), 152.86 (phenyl *C*-1), 155.78 (*C*=O). HRMS, calculated for $C_{11}H_{14}N_2O_4$ 238.0954, found 238.0959.

*2,4-Di-tert-butylphenyl-N-butylcarbamate (**10**).* ^{1}H NMR ($CDCl_3$, 400 MHz), δ (ppm) 0.95 (t, $J = 7$ Hz, 3H, $CH_2CH_2CH_3$), 1.32 [s, 9H, *o*-$C(CH_3)_3$], 1.38 [s, 9H, *p*-$C(CH_3)_3$], 1.38 (sextet, $J = 7$ Hz, 2H, $CH_2CH_2CH_3$), 1.55 (quintet, $J = 7$ Hz, 2H, $CH_2CH_2CH_3$), 3.29 (q, $J = 7$ Hz, 2H, $NHCH_2$), 5.01 (br s, 1H, N*H*), 6.95–7.36 (m, 3H, aromatic *H*). ^{13}C NMR ($CDCl_3$, 100 MHz), δ (ppm) 13.84 ($CH_2CH_2CH_3$), 19.98 ($CH_2CH_2CH_3$), 30.42 [*o*-$C(CH_3)_3$], 31.59 [*p*-$C(CH_3)_3$], 32.12 ($CH_2CH_2CH_3$), 34.69 [*o*-$C(CH_3)_3$], 34.78 [*p*-$C(CH_3)_3$], 41.04 ($NHCH_2$), 123.27, 123.54, 123.71 (phenyl *C*H), 139.99 (phenyl *C*-2), 146.92 (phenyl *C*-4), 147.31 (phenyl *C*-1), 154.61 (*C*=O). HRMS, calculated for $C_{19}H_{31}NO_2$ 305.2355, found 305.2358.

*Phenyl-N-butylcarbamate (**11**).* ^{1}H NMR ($CDCl_3$, 400 MHz), δ (ppm) 0.96 (t, $J = 7$ Hz, 3H, $CH_2CH_2CH_3$), 1.35 (sextet, $J = 7$ Hz, 2H, $CH_2CH_2CH_3$), 1.56 (quintet, $J = 7$ Hz, 2H, $CH_2CH_2CH_3$), 3.27 (q, $J = 7$ Hz, 2H, $NHCH_2$), 4.99 (br s, 1H, N*H*), 7.12–7.37 (m, 4H, aromatic *H*). ^{13}C NMR ($CDCl_3$, 100 MHz), δ (ppm) 13.81($CH_2CH_2CH_3$), 19.99 ($CH_2CH_2CH_3$), 31.96 ($CH_2CH_2CH_3$), 41.00 ($NHCH_2$), 121.42 (phenyl *C*-3, *C*-5), 125.00 (phenyl *C*-4), 129.05 (phenyl *C*-2, *C*-6), 150.89 (phenyl *C*-1), 154.37 (*C*=O). HRMS, calculated for $C_{11}H_{15}N_2O_4$ 193.1103, found 193.1104.

Acknowledgment

We thank the National Science Council of Taiwan for financial support.

REFERENCES

1. Brockerhoff H, Jensen RG. *Lipolytic Enzymes*. Academic Press: New York, 1974.
2. Kritchevsky D, Kothari HV. *Adv. Lipid Res.* 1978; **16**: 221–226.
3. Rudd EA, Brockman HL. *Lipases*. Elsevier: Amsterdam, 1984.
4. Wang X, Wang C-S, Tang J, Dyda F, Zhang XC. *Structure* 1997; **5**: 1209–1218.
5. Chen JC-H, Miercke LJW, Krucinski J, Starr JR, Saenz G, Wang X, Spilburg CA, Lang LG, Ellworth JL, Stround RM. *Biochemistry* 1998; **37**: 5107–5117.
6. Theil F. *Chem. Rev.* 1995; **95**: 2203–2227.
7. Lang DA, Mannesse MLM, De Haas GH, Verheij HM, Dijkstra BW. *Eur. J. Biochem.* 1998; **254**: 333–340.
8. Grochulski P, Bouthillier F, Kazlauskas RJ, Serreqi AN, Schrag JD, Ziomek E, Cygler M. *Biochemistry* 1994; **33**: 3494–3500.
9. Bhat SG, Brockman HL. *Biochem. Biophys. Res. Commun.* 1982; **109**: 486–492.
10. Gallo LL, Clark SB, Myers S, Vohouny GV. *J. Lipid Res.* 1985; **25**: 604–612.
11. Scheen AJ. *Rev. Med. Liege*. 1999; **54**: 707–709.
12. Heck AM, Yanovski JA, Calis KA. *Pharmacotherapy* 2000; **20**: 270–279.
13. Brodt-Eppley J, White P, Jenkins S, Hui DY. *Biochim. Biophys. Acta* 1995; **1272**: 69–72.
14. Svendsen A. In *Lipases, Their Structure Biochemistry and Application*. Cambridge University Press: Cambridge, 1994.
15. Hosie L, Sutton LD, Quinn DM. *J. Biol. Chem.* 1987; **262**: 260–264.

16. Lin G, Lai C-Y. *Tetrahedron Lett.* 1995; **36**: 6117–6120.
17. Lin G, Lai C-Y. *Tetrahedron Lett.* 1996; **37**: 193–196.
18. Feaster SR, Lee K, Baker N, Hui DY, Quinn DM. *Biolchemistry* 1996; **35**: 16723–16734.
19. Lin G, Tsai Y-C, Liu H-C, Liao W-C, Chang C-H. *Biochim. Biophys. Acta* 1998; **1388**: 161–174.
20. Lin G, Shieh C-T, Ho H-C, Chouhwang J-Y, Lin W-Y, Lu C-P. *Biochemistry* 1999; **38**: 9971–9981.
21. Lin G, Lai C-Y, Liao W-C, Kuo B-H, Lu C-P. *J. Chin. Chem. Soc.* 2000; **47**: 489–500.
22. Lin G, Chouhwang J-Y. *J. Biochem. Mol. Biol. Biophys.* 2001; **5**: 301–308.
23. Aldridge WN, Reiner E. In *Enzyme Inhibitors as Substrates*, Neuberger A, Tatun EL (eds). North-Holland: Amsterdam, 1972; 123–145.
24. March J. *Advanced Organic Chemistry* (4th edn). Wiley: New York, 1992.
25. Isaacs N. *Physical Organic Chemistry* (2nd edn). Longman: Harlow, 1995.
26. Lowry TH, Richardson KS. *Mechanism and Theory in Organic Chemistry* (3rd edn). Harper and Row: New York, 1992.
27. Fujita T, Nishioka T. *Prog. Phys. Org. Chem.* 1976; **12**: 49–89.
28. Lin G. *J. Phys. Org. Chem.* 2000; **13**: 313–321.
29. Lee I. *Adv. Phys. Org. Chem.* 1992; **27**: 57–117.

